Internal Atmospheric Dynamics and Tropical Indo-Pacific Climate Variability

Ben P. Kirtman[1,2], Kathy Pegion[1] and Saul M. Kinter[2]

[1]George Mason University, Fairfax Virgina
[2]Center for Ocean-Land-Atmosphere Studies
4041 Powder Mill Road, Suite 302
Calverton, MD 20705

e-mail:kirtman@cola.iges.org

Abstract

One possible explanation for tropical sea surface temperature (SST) interannual variability is that it can be accurately described by a linear auto-regressive model with damped coupled feedbacks and stochastic forcing. This auto-regressive model can be viewed is a "null hypothesis" for tropical SST variability. This paper advances a new coupled general circulation model (CGCM) coupling strategy, called an interactive ensemble as a method to test this null hypothesis. The design of the interactive ensemble procedure is to reduce the stochastic variability in the air-sea fluxes applied to the ocean component while retaining the deterministic component of the coupled feedbacks. The interactive ensemble procedure uses multiple realizations of the atmospheric GCM coupled to a single realization of the ocean GCM. The ensemble mean of the atmospheric GCM fluxes are applied to the ocean model thereby significantly reducing the variability due to internal atmospheric dynamics in the air-sea fluxes. If the null hypothesis is correct, the SST variability is reduced, and the auto-regressive model defines how much the variability should be reduced. In order to test the null hypothesis, we apply the interactive ensemble procedure to a heuristic coupled model. We then use the heuristic coupled model to interpret the CGCM interactive ensemble results with respect to: (i) SST variance and (ii) how the amplitude of atmospheric internal dynamics depends on the evolving background SST anomaly. There are significant regions where the heuristic model fails to reproduce the CGCM results, suggesting that aspects of tropical Indo-Pacific variability *in the CGCM* cannot be explained by damped coupled feedbacks and stochastic forcing. These regions are largely coincident with regions of large convective anomalies. Surprisingly, we also find significant regions in the tropical eastern Pacific where the variability due to internal ocean dynamics cannot be neglected.

1. Introduction

There is currently a debate regarding the processes that ultimately limit the predictability of the El Niño-Southern Oscillation (ENSO). According to this debate, ENSO may be in one of three regimes. In first regime, ENSO is intrinsically chaotic due to the non-linear dynamics of the coupled system (Zebiak and Cane 1986; Munnich et al. 1991; Jin et al. 1994; Chang et al. 1994; Zebiak 1989; Tziperman et al. 1995; Wang et al. 1999). The loss of predictability is primarily due to the uncertainty in the initial conditions. In the second regime, ENSO is self-sustained (due to weak non-linearity) and is periodic, i.e., perfectly predictable (Battisti, 1988; Suarez and Schopf 1988; Jin 1997; Kirtman, 1997). The irregularity of ENSO is due to external weather noise (e.g., Kirtman and Schopf 1998; Eckert and Latif 1997; Blanke et al. 1997) and the loss of predictability is primarily due to this external stochastic forcing. In the third regime, ENSO is damped and stochastically forced by external weather noise (Penland and Matrosova, 1994; Penland and Sardeshmukh, 1995; Flugel and Chang 1996; Moore and Kleeman 1996; Kleeman and Moore 1997; Thompson and Battisti, 2001; Moore and Kleeman 1999a; 1999b; Flugel et al., 2004). The non-normality of the coupled system allows for limited time super-exponential perturbation growth (e.g., Xue et al. 1997; Chen et al. 1997; Moore and Kleeman 1999a; Thompson and Battisti 2000; Kleeman et al. 2003). Here the predictability is limited either by the stochastic forcing exciting these optimally growing modes, or by initial errors efficiently projecting onto the optimally growing modes.

From the perspective of making ENSO predictions with state-of-the-art coupled general circulation models (CGCMs), it is not obvious whether it matters which regime is correct. Presumably, the CGCM includes the possibility of all three regimes. On the other hand, the limit of ENSO predictability is highly dependent on which regime is correct. For example, Thompson and

Battisti (2001) showed that, in the damped regime, the limit of predictability was on the order of 9-15 months, whereas in the chaotic regime the limit was considerably longer (15-24 months). Thompson and Battisti (2001) went on to argue that the damped stochastically forced model did the best job at reproducing the observed ENSO statistics, although it is unclear how this result is affected by the limitations in the simplified model physics. Kirtman and Schopf (1998) used a model that primarily resides in the self-sustained and stochastically forced regime to argue that ENSO vacillates between highly predictable regimes (oscillatory and self-sustained) and periods of low predictability when the variability is driven by the noise. Whether the model resides in the predictable or the unpredictable regime is determined by low frequency variability in the background state (Federov and Philander, 2001). Conversely, Flugel et al. (2004) used a model that entirely resides in the damped regime to argued that the background state changes are merely a sampling issue and that the changes in predictability are associated with how the stochastic forcing projects onto the optimals. In this case, variations in predictability are a random walk process. Determining which regime dominates in Nature is also important from the prospective of designing observing systems and model improvement strategies.

The debate continues in part because most of our understanding is based on relatively simple models that include stochastic processes in an ad-hoc manner and/or oversimplify the non-linear dynamics and coupling. The relative importance of stochastic forcing versus deterministic coupling has not been analyzed within the context of CGCMs, let alone Nature. Here we emply a new coupling strategy, called interactive ensembles, that has been developed specifically to examine the relative importance of stochastic forcing and deterministic coupling in generating climate variability in CGCMs (Kirtman and Shukla 2002). The interactive ensemble strategy is to couple multiple realizations of a particular atmospheric GCM (AGCM) to a single oceanic GCM (OGCM). Ensemble averaging is applied to the air-sea fluxes of heat, momentum and fresh water thereby significantly reducing the "noise" in the fluxes applied to the ocean component without affecting the atmospheric internal dynamic fluctuations that are unrelated to the SST anomalies (SSTA). This approach is distinct from *a posteriori* ensemble averaging of multiple coupled model realizations, because the ensemble averaging is applied to the atmospheric fluxes as the coupled system evolves, and is, therefore, viewed as fully interactive. It is important to note that atmospheric noise is part of the real climate system, and we are not arguing that removing the noise is an appropriate mechanism for directly improving the simulation. We are, however, advocating a unique experimental strategy for determining how noise impacts climate variability, and by reducing the interference due to the noise, increasing our understanding of the mechanisms associated with deterministic coupled air-sea feedbacks. Indirectly, this increased understanding will help improve climate models and their simulations.

Kirtman and Shukla (2002), in a "proof of concept" paper, compared multi-century simulations from a six-member version of the interactive ensemble with a control simulation (Kirtman et al., 2002) using one realization of the Center for Ocean-Land-Atmosphere Studies atmospheric model (COLA AGCM) coupled to the ocean component consisting of the Geophysical Fluid Dynamics Laboratory Modular Ocean Model (GFDL-MOM3; Pacanowski and Griffies 1998). Their analysis suggested that: (i) the noise reduction only slightly decreases the amplitude of the ENSO oscillation, shortens the periodicity and increases the regularity, and (ii) the global ENSO SST teleconnections and ENSO-monsoon interactions are highly sensitive to the amplitude of the stochastic forcing. Yeh and Kirtman (2004a; 2004b) used the interactive ensemble approach to diagnose SST variability in the North Pacific, arguing that local stochastic forcing dominated much of the variability and masked out the mid-latitude tropical SST teleconnections on interannual time scales.

Yeh and Kirtman (2004c) examined the relationship between low frequency (decadal) variability in the tropical mean state and ENSO variance using the interactive ensemble. They found two important "modes" of tropical decadal variability. The first mode explains approximately 40% of the tropical low frequency variability, has basin scale, is unrelated to low frequency variations of ENSO amplitude, and appears to be forced by atmospheric noise, although precisely how the noise preferentially excites this mode remains to be determined. This first mode is consistent with the theory that ENSO is linear, damped and stochastically forced, suggesting that changes in the tropical mean state (associated with this first mode) and ENSO variance are due to sampling issues. This linear damped stochastic theory for ENSO is often viewed as the "null hypothesis" (Flugel et al., 2004) and is discussed in detail in Section 3. On the other hand, the second mode (~15% of the variance) was found to be unambiguously correlated to low frequency changes in ENSO variance, demonstrating that there is a component of the ENSO variability that cannot be explained by the damped linear theory.

Traditionally, ensembles of atmospheric realizations have been used to isolate forced SST climate signals and filter the noise due to internal atmospheric dynamics. The interactive ensemble coupling strategy generalizes this use of atmospheric ensembles to free running long coupled climate simulations. In other words, the approach can be used to isolate the deterministic coupled signal within the context of a long coupled simulation. For example, Wu and Kirtman (2003) took advantage of the interactive ensemble approach to separate ENSO-related and –unrelated Indian summer monsoon variability in a 500-yr coupled CGCM simulation. They found that ENSO-related monsoon variability has significant impacts on the subsequent evolution of warm events. The mechanism was found to be similar to that described by Kirtman and Shukla

(2000). Similarly, Wu and Kirtman (2004a; 2004b) exploited the interactive ensemble approach to isolate the importance of coupled air-sea feedbacks over warm tropical oceans for monsoon-global ocean teleconnections.

The purpose of this paper is to provide a more basic understanding of how noise due to internal atmospheric dynamics impacts SST variability in the tropical Indo-Pacific region. In order to do this, we describe a heuristic coupled model and apply the interactive ensemble strategy to the heuristic model, which is then used to interpret the results from the CGCM version of the interactive ensemble. The heuristic model is not particularly new; however, it provides a mechanism for understanding how the interactive ensemble is implemented and a framework for how to interpret the interactive ensemble results. The basic idea for the heuristic model is a generalization of the Barsugli and Battisti (1998) model applied to tropical SST variability. The model assumes linear damped coupled feedbacks where both the ocean and atmosphere are forced by stochastic variability. The inclusion of ocean stochastic forcing is distinct from Battisti and Barsugli and is motivated by Wu et al. (2004) who found that ocean internal dynamics can have a significant impact on SST variability in the North Atlantic. First we describe the heuristic coupled model and how the interactive ensemble is applied. We then use the heuristic coupled model to interpret the CGCM interactive ensemble results with respect to: (i) SST variance and (ii) the dependence of the amplitude of atmospheric internal dynamics on the evolving background SSTA. There are significant regions where the heuristic model fails to reproduce the CGCM results, suggesting that aspects of tropical Indo-Pacific variability *in the CGCM* cannot be explained by damped coupled feedbacks and stochastic forcing. Typically, these regions are associated with tropical convection, which leads to the conjecture that the heuristic model does not include some non-linearities that are fundamental to the coupled system and cannot be accurately modeled as linear Gaussian white noise. This result also supports the Yeh and Kirtman (2004c) findings regarding the low frequency modulation of ENSO.

2. Models and Coupling Strategies

The anomaly coupled GCM (ACGCM) combines the COLA atmospheric GCM and the Geophysical Fluid Dynamics Laboratory (GFDL) Modular Ocean Model (MOM), version 3.0. Brief descriptions of these models and the coupling procedures are given below. Details of how well the model performs in long climate simulations are described in detail in Kirtman et al. (2002).

a. Atmospheric Model

A number of changes to the atmospheric model have been made since the original coupled models were developed. The dynamic core used in the National Center for Atmospheric Research (NCAR) Community Climate Model (CCM) version 3.0 has been adopted (Schneider, 2001). The dynamic core is spectral (triangular truncation at total wavenumber 42) with semi-Lagrangian transport. There are 18 unevenly spaced Φ-coordinate vertical levels. The parameterization of the solar radiation is after Briegleb (1992) and terrestrial radiation follows Harshvardhan et al. (1987). The deep convection is an implementation of the Relaxed Arakawa-Schubert (RAS) scheme of Moorthi and Suarez (1992) described by DeWitt (1996). The convective cloud fraction follows the scheme used by the NCAR CCM (Kiehl et al., 1994; see DeWitt and Schneider, 1996 for additional details). The model includes a turbulent closure scheme for the subgrid scale exchange of heat, momentum, and moisture after Miyakoda and Sirutis (1977) and Mellor and Yamada (1982). Additional details regarding the AGCM physics can be found in Kinter et al. (1988) and DeWitt (1996). Model documentation is given in Kinter et al. (1997).

b. Ocean Model

The ocean model is version 3 of the GFDL MOM (Pacanowski and Griffies, 1998), a finite-difference treatment of the primitive equations of motion using the Boussinesq and hydrostatic approximations in spherical coordinates. The domain is that of the world ocean between 74^{o}S and 65^{o}N. The coastline and bottom topography are realistic except that ocean depths less than 100 m are set to 100 m and the maximum depth is set to 6000 m. The artificial high-latitude meridional boundaries are impermeable and insulating. The zonal resolution is 1.5^{o}. The meridional grid spacing is 0.5^{o} between 10^{o}S and 10^{o}N, gradually increasing to 1.5^{o} at 30^{o}N and 30^{o}S and fixed at 1.5^{o} in the extratropics. There are 25 levels in the vertical with 17 levels in the upper 450 m. The vertical mixing scheme is the non-local K-profile parameterization of Large et al. (1994). The horizontal mixing of tracers and momentum is Laplacian. The momentum mixing uses the space-time dependent scheme of Smagorinsky (1963) and the tracer mixing uses Redi (1982) diffusion along with Gent and McWilliams (1990) quasi-adiabatic stirring.

c. Coupling Strategy

The anomaly coupling strategy is described in detail in Kirtman et al. (1997) and in Kirtman et al. (2002). The main idea is that the ocean and atmosphere exchange predicted anomalies, which are computed relative to their own model climatologies, while the climatology upon which the anomalies are superimposed is specified from observations. The anomaly coupling strategy requires atmospheric model climatologies of momentum, heat and fresh water flux, and an ocean model SST climatology. Similarly, observed climatologies of momentum, heat and fresh water flux and SST are also required. The model climatologies are defined by separate uncoupled extended simulations of the ocean and atmospheric models. In the case of the atmosphere, the model climatology is computed from a 30 year (1961-1990) integration with specified observed SST and sea ice. This SST is also used to define the observed SST climatology. In the case of the ocean model SST climatology, an extended uncoupled ocean model simulation is made using 30 years of 1000 mb winds from the National Centers for Environmental Prediction (NCEP) reanalysis (Kalnay et al. 1996). The NCEP winds are converted to a wind stress following Trenberth et al. (1990). As with the SST, this observed wind stress product is used to define the observed momentum flux climatology. The heat flux and the fresh water flux in this ocean-only simulation is parameterized by damping SST and sea surface salinity to observed values with a 100-day time scale. The heat and fresh water flux “observed” climatologies are then calculated from the results of the extended ocean-only simulation. The ocean and atmosphere model exchange daily mean fluxes and SST once a day.

d. The Interactive Ensemble Technique

Figure 1 shows a schematic representation of an application of the interactive ensemble technique. The AGCM is identical for each ensemble member and the AGCM realizations only differ in their initial conditions. Because the atmosphere is sensitively dependent on initial conditions, the AGCM realizations evolve differently. As the interactive ensemble evolves, each AGCM realization experiences the same SST predicted by the OGCM. The OGCM, on the other hand, experiences surface fluxes of heat, momentum and freshwater that are the ensemble average of the AGCM realizations. The AGCM realizations are noise independent (i.e., the noise among the ensemble members in uncorrelated), but since they are all coupled to the same SST, they have the same signal. The models are fully interactive in that the component models exchange fluxes and SST once a day.

It is our assertion that the behavior of the interactive ensemble coupled model is different from that obtained by simply time averaging the AGCM fluxes at the air-sea interface as a traditional coupled model (i.e., one atmosphere coupled to one ocean) evolves. This assertion is based on the intuition that the ergodic hypothesis begins to break down for short time averages and small ensemble sizes. It is reasonable that, *with fixed boundary conditions*, relatively large ensembles and long time averages yield similar results; however, in the coupled model the boundary conditions are evolving and time averages are not equivalent to ensemble averages. Is the six-member ensemble mean, for example, significantly different from the six-day time mean of any particular ensemble member as the boundary conditions evolve? To address this question we have plotted (Fig. 2) the zonal wind stress variance of six-day means for three particular ensemble members chosen at random (dashed curves) and for the ensemble mean (solid curve) of six ensemble members. The variance plotted in Fig. 2 is calculated over time (1-year) as the deviation about the annual cycle. The structure of the variance of the ensemble mean is substantially different from any of the ensemble members suggesting that we would not expect similar results by only time filtering on this time scale. Even with 12-day means and 12-member ensembles there are substantial differences in the variances (not shown), with longer time averaging the signal becomes seriously degraded. In fact, there may be relatively high frequency variability that is coupled to the SST that would be filtered by the time averaging and not by the ensemble averaging. Intraseasonal variability is one possible example of such a phenomenon (Waliser et al., 1999, Leiss et al., 2001; Wang and Xie 1997), although this is the subject of some debate.

Two multi-century coupled simulations are presented here. The first is a control simulation in which one atmosphere is coupled to one ocean. The second simulation is a six-member version of the interactive ensemble applied to the same atmospheric component. Both simulations were run for over 300 years, and the last 100-years of each simulation were analyzed. We have examined different samples of the coupled model results and have found little sensitivity in the basic results shown here. The results are also entirely consistent with a twelve-member version of the interactive ensemble.

3. Heuristic Coupled Model and the Interactive Ensemble

In this section we present a heuristic coupled model and apply the interactive ensemble strategy to the model. The model serves two purposes. First, it is instructive in terms of understanding how the interactive ensemble strategy is implemented. Second, the heuristic model is, in some sense, a null hypothesis for tropical Indo-Pacific SST variability that can be used to interpret the interactive ensemble as it is applied to the CGCM. Simply, the heuristic model describes what to expect if we assume that the SST variability is accurately modeled by damped coupled feedbacks and linear stochastic forcing. While this formalism is not particularly new, it indicates that the role of ocean internal dynamics cannot be neglected. In order to clarify how the noise reduction in the interactive ensemble works, we briefly discuss atmospheric ensemble realizations as they relate to the interactive ensemble procedure. We then apply the interactive ensemble to the heuristic coupled model and compare the results with the CGCM.

a. Atmospheric Ensembles

For any atmospheric realization, assume that any field at any point in space and time can be written as $X_k=X_s+N_k$ where X_k refers to the k^{th} ensemble member, X_s is the undetermined signal and N_k is the undetermined noise due to internal atmospheric dynamics. The noise associated with each ensemble member is uncorrelated with the noise in any other ensemble member and the temporal variance (σ_N^2) of all the noise realizations are the same. The noise has zero mean. It is assumed that each atmospheric ensemble member experiences the same surface boundary conditions. The ensemble mean is defined as

$$X_e = X_s + \frac{1}{M}\sum_{k=1}^{M} N_k \qquad (1)$$

for M atmospheric ensemble members. The signal (X_s) is then defined as the limit of the ensemble mean as the ensemble size (M) goes to infinity. With this definition of the signal, the noise in any realization (N_k) is also defined. In practical applications with AGCMs, the signal and the noise due to internal dynamics can only be approximated - we do not have infinite ensembles. It should also be noted that for any finite ensemble size and at any point in space or time, the ensemble mean (X_e) has non-zero noise. The internal dynamics noise of the ensemble mean is

$$\varepsilon = \frac{1}{M}\sum_{k=1}^{M} N_k \tag{2}$$

which converges to zero as the ensemble size becomes infinite.

Define the ensemble spread (S) at any point in space and time as

$$S = \frac{1}{M}\sum_{k=1}^{M} (X_e - X_k)^2 \tag{3}$$

which can be written as

$$S = \frac{1}{M}\sum_{k=1}^{M} N_k^2 - \varepsilon^2 \tag{4}$$

For a finite ensemble, the ensemble spread (S) is an estimate, albeit an underestimate, of the mean squared noise ($\frac{1}{M}\sum_{k=1}^{M} N_k^2$) in the ensemble. We will return to the issue of the ensemble spread when we compare the heuristic model and the CGCM results. The key point here is that with finite ensemble sizes, there is noise in the ensemble mean and this ensemble mean noise influences the ensemble spread.

b. SSTA Variance Ratios

In the following we demonstrate how the interactive ensemble approach can be applied to a simple stochastic coupled model. The approach is to use a simplified version of the model used by Barsugli and Battisti (1998) with the addition of internal dynamics noise in the ocean component. For the standard coupled model (i.e., one atmosphere coupled to one ocean), we assume

$$\begin{aligned} X^{n+1} &= \alpha Y^n + \gamma X^n + N \\ Y^{n+1} &= \beta X^n + \delta Y^n + P \end{aligned} \tag{5}$$

where X is viewed as the atmospheric component and Y is the ocean component. The memory of the previous state (i.e., *uncoupled* lag-1 auto-correlation) is given by the γ and δ terms. The variables N and P represent uncoupled or internal noise in the component models, which is assumed to be Gaussian and white. The coupling coefficients are bounded between zero and one, and if ∀□∃, then the model is non-normal. A similar model was used by Yeh and Kirtman (2004a), but without the lag-one auto-correlation terms.

This simple coupled model can easily be generalized into an interactive ensemble version. Here we assume M atmospheric models coupled to one ocean model as follows.

$$\begin{aligned} X_1^{n+1} &= \alpha Y^n + \gamma X_1^n + N_1 \\ &\dots \\ X_M^{n+1} &= \alpha Y^n + \gamma X_M^n + N_M \\ Y^{n+1} &= \frac{\beta}{M}\sum_{k=1}^{M} X_k^n + \delta Y^n + P \end{aligned} \tag{6}$$

The coupled feedbacks and the uncoupled lag-1 auto-correlation are the same as in the control model (5). Since the noise statistics are the same for each ensemble member, they are statistically indistinguishable from each other. Each atmospheric component model is also statistically indistinguishable from the control model up to the changes in the variance in the ocean component. Indeed, it is the change in the variance of the ocean components we wish to compute. In some sense, comparing the variance of the ocean component of (5) and (6) provides the null hypothesis for analyzing the changes in SST variance in applying the interactive ensemble procedure to the

CGCM. In other words, if the climate system behaves in a manner that is accurately described by damped linear stochastically forced dynamics, what changes in ocean variance do we expect from application of the interactive ensemble?

The changes in the expected variance ratio for various values of the coupling strength and as a function of the ratio of ocean internal noise divided by atmospheric internal noise (σ_P^2 / σ_N^2) are plotted in Fig. 3. Here we have assumed a six-member ensemble, and that the ocean uncoupled lag-1 (i.e., one month) auto-correlation is 0.75 and the atmospheric uncoupled lag-1 auto-correlation is 0.25. We have computed the variance ratios for a wide range of values of γ and δ and have found little sensitivity. For weak coupling, the variance ratio becomes relatively large for relatively small values of ocean noise. If the coupling is weak, then the ocean noise has a large effect on the variance. As the coupling strength increases, the variance ratio approaches one only with considerably larger values of the ocean noise. In this case, the coupling is more important and the ocean noise has a smaller impact. Regardless of the coupling strength (as long as it is damped) the variance ratio is bounded by 1.0 independent of the relative amplitudes of the ocean and atmosphere noise.

In order to interpret the CGCM results presented in Fig. 4 described below, it is useful to consider three ranges of values for the ratio of the SST variances. These values are chosen qualitatively based on the results presented in Fig. 3. (i) If the SST variance ratio is on the order of 0.2, we conclude that the null hypothesis is likely to be correct (i.e., a stochastically forced system with stable coupled feedbacks) and *the ocean noise is relatively small*. (ii) If the SST variance ratio is between 0.5 and 1.0 then either the null hypothesis is correct and the ocean noise is playing a significant role or the null hypothesis is incorrect and there are unstable coupled feedbacks or important non-linearities. In other words, additional experiments are needed to isolate the role of the ocean noise. (iii) If, on the other hand, the ratio exceeds 1.0, then the variability in the CGCM cannot be explained by the damped, linear model and there must be unstable coupled feedbacks and/or important non-linearities.

The SSTA variance from the control CGCM run in the Indo-Pacific region is shown in Fig. 4a and the SSTA variance ratio of the CGCM interactive ensemble to the control is shown in Fig. 4b. Using the heuristic model results as a guide, we conclude that there are substantial regions in the western and central tropical Pacific and the eastern south tropical Indian Ocean where there are unstable coupled feedbacks and non-linearity. In the un-shaded regions, there may be some contribution due to the internal ocean dynamics, but the coupled feedbacks are unlikely to be unstable. Figure 4b also shows that there are surprisingly large regions, particularly in the eastern Pacific, where noise due to *internal ocean dynamics* cannot be eliminated as a contributor to the SST variability. Despite the fact that the ocean model is not eddy resolving, it produces noise due to internal ocean dynamics (i.e., transients), although the statistics are likely to have significant errors due, in part, to relatively low ocean resolution. One possible explanation for the results in the eastern Pacific is that tropical ocean instability waves, albeit poorly represented, are making a significant contribution to the SSTA variability.

Finally it is also worth noting that the heuristic model used here is non-normal only when coupled. The individual uncoupled atmospheric and oceanic component models are normal. This is not necessarily the case with other more physically based “null hypothesis” models, such as the model used by Moore and Kleeman (1999a). However, the Battisti and Thompson (2000) model only has one non-normally growing mode (i.e., due to coupled interactions) suggesting that the non-normality of the uncoupled individual component model will not impact the qualitative nature of the results discussed here.

c. Ensemble Spread and Ensemble Mean

As a second test of the null hypothesis, this section examines the relationship between the ensemble mean (1) and the ensemble spread (3) within the context of the interactive ensemble. We show here that there is no relationship between the ensemble spread and the ensemble mean in the heuristic interactive ensemble coupled model. This is, perhaps, conceptually clear given that the noise is externally prescribed. On the other hand, if a robust relationship exists between the two in the CGCM, this not only suggests that the null hypothesis is inconsistent with the CGCM, but also has implications for predictability. Suppose, for example, that atmospheric wind stress uncertainty (i.e., spread) is dependent on the anomalous state of the tropical Pacific Ocean, so that the uncertainty is larger for warm events. This would suggest that warm events are less predictable than cold events. In fact, this is shown for the CGCM below, which is also borne out in retrospective ENSO predictions (i.e., Kirtman 2003), and which cannot be reproduced by the damped linear model.

As with the ratio of variances shown in Figs. 3 and 4, we first consider what is the expected relationship between the ensemble mean and spread assuming that the variability is accurately described by the heuristic model. The heuristic model results, calculated using (6), are summarized in Fig. 5. Figure 5a shows the probability density function (pdf) for the ensemble mean atmospheric state (red curve) and the ensemble spread (black curve). The pdfs are plotted in terms of frequency or percent occurrence along the y-axis and as a function of their respective standard deviations along the x-axis. As expected the ensemble mean atmospheric state is nearly Gaussian and the ensemble spread has a skewed distribution. The spread pdf is calculated with respect to the long-term mean spread. Figure 5a also shows the conditional pdf of the ensemble spread (blue curve) assuming that the ensemble mean is at least one standard deviation above normal. The total spread pdf and the *conditional* spread pdf are virtually indistinguishable indicating that there is no relationship between the ensemble mean and the ensemble spread. For the sake of completeness, Fig. 5b shows the conditional (condition based on ensemble spread) ensemble mean pdf compared to the total ensemble mean pdf. As with the spread, the two ensemble mean pdfs are indistinguishable.

The analogous results from the interactive ensemble CGCM are presented in Fig. 6. Here we have used the zonal wind stress anomalies in the Nino4 region to calculate the ensemble mean and ensemble spread pdfs. In Figs. 6a-b, the ensemble mean pdf (red curve) also appears to be nearly Gaussian although this has not been tested. The ensemble spread pdf (black curves in Figs. 6a-b) is skewed, but considerably less than with the heuristic model. The conditional pdf for the ensemble spread is shown in blue in both Figs 6a-b. In this case we show the conditional spread pdf when the ensemble mean is at least one standard deviation below normal (Fig. 6a) and when the ensemble mean is at least one standard deviation above normal (Fig. 6b). Figure 6a indicates that when there are strong easterly anomalies in the ensemble mean, the spread is typically anomalously small – the atmospheric uncertainty is relatively small. Conversely, when there are westerly anomalies in the ensemble mean (Fig. 6b), the atmospheric uncertainty is relatively large. As stated earlier, this feature is not present in the null hypothesis model.

Figures 7a-b show the pdfs from a slightly different perspective. Here we examine unconditional and conditional SSTA (averaged in the Nino3.4 region) assuming relatively small zonal wind stress spread (Fig. 7a) and relatively large zonal wind stress spread (Fig. 7b). As with the heuristic model, the conditional distributions are based on plus (or minus) one standard deviation of the zonal wind stress spread. The unconditional SSTA pdf (red curve) appears to be

Gaussian. The conditional SSTA pdf (Fig. 7a, blue curve) for small zonal wind stress spread shows a clear shift to an increased probability of a cold event. In fact, the probability of a warm event is negligible. When the spread is relatively large the probability of warm events is significantly enhanced, although there is a non-zero probability of weak cold events.

The fact that the unconditional SSTA is Gaussian (i.e., red curves in Figs. 7a-b) is worth further comment. It is straightforward to tune the heuristic model to reproduce the SSTA pdf from the CGCM, but the heuristic model cannot reproduce the conditional pdfs. A SSTA Gaussian pdf does not necessarily imply that the dynamics and physics of the coupled system can be accurately simulated by a damped, linear, and stochastically forced model, because there may be important non-linearity that cannot be detected by examining just one variable.

The spatial distribution of the conditional pdfs are summarized in Figs. 8a-d using a conditional composite approach. For example, Fig. 8a shows the mean spatial distribution of the top 5% of all warm events (measured by Nino3.4 SSTA) and Fig. 8b is the mean spread of the zonal wind stress anomaly using the same 5% of all warm events. Similarly, Fig. 8c shows the top 5% of all cold events and the corresponding composite of the zonal wind stress anomaly is shown in Fig. 8d. As with Figs. 6-7, the spread is relatively large for warm events and relatively small for cold events. Figure 8 also suggests that changes in the spread are primarily associated with changes in the amplitude without much change in the spatial structure. For example, Fig. 8b and 8d indicate that the amplitude of the spread decreases uniformly during large cold events.

The fact that there are relatively small changes in the spatial structure of the spread suggests that the spatial structure of the noise has an important aspect. To demonstrate this point we show the first empirical orthogonal function (EOF) of the ensemble mean zonal wind stress anomaly (Fig. 9a) and the first EOF of the zonal wind stress anomaly deviation about the ensemble mean. Figure 9a shows the dominant structure in the deterministic coupled “signal,” and the Fig. 9b shows the dominant structure of the atmospheric uncertainty or noise. The structure of the atmospheric uncertainty occurs on relatively large scales and is quite similar to the signal. The primary uncertainty is in terms of the amplitude of the signal; the spatial structure in the uncertainty is of secondary importance. Figure 9 also shows that the use of the term noise incorrectly connotes relatively small scales. The noise occurs on all scales with perhaps the most important scale being the largest.

4. Concluding Remarks

The null hypothesis for tropical SSTA variability is that this variability is accurately described by a linear auto-regressive model that has damped coupled feedbacks and is stochastically forced (e.g., Thompson and Battisti 2001; Flugel et al. 2004). Testing this null hypothesis in simplified coupled models is fairly straightforward, but has not been done for CGCMs. In this paper, we show that a new coupling strategy that can be used to test this null hypothesis within the context of a CGCM. The coupling strategy, called an interactive ensemble, is specifically designed to reduce the noise in air-sea fluxes that are exchanged with the ocean component, thereby significantly reducing the stochastic forcing from the atmosphere. If the null hypothesis is correct, we expect the CGCM variability to be correspondingly reduced when the interactive ensemble strategy is applied.

In order to test this null hypothesis, we formulated a heuristic coupled model (auto-regressive, damped coupled feedbacks and stochastically forced) for comparison with the CGCM. As recommended by Wu et al. (2004), we included stochastic forcing for the ocean component. We then applied the interactive ensemble approach to both the heuristic model and the CGCM and compared the SSTA variance ratios (i.e., the variance in the interactive ensemble model divided by that in the standard coupled model) produced by the heuristic model and by CGCM. We found that there are large regions in the western and central tropical Pacific and the eastern south tropical Indian Ocean where the null hypothesis could not explain the changes in the variability. These regions coincide with large convective anomalies suggesting the importance of non-linearity. There are also large regions, particularly in the eastern Pacific, where *internal ocean dynamics* cannot be eliminated as a significant contributor to the SST variability. We speculate that tropical instability waves may be making a significant contribution to the variability in this region. The potential importance of internal ocean dynamics indicates that the interactive ensemble procedure also needs to be expanded to include the ocean component.

One of the by-products of the interactive ensemble strategy is that there is an ensemble of atmospheric states that are consistent with the SST, and that can be used to diagnose the variability. We were specifically interested in the relationship between the ensemble mean and the ensemble spread, if any. Similar to the analysis of variance, we used the heuristic model as a guide for what to expect from the null hypothesis and for comparison with the CGCM results. According to the null hypothesis, there can be no relationship between the spread and the ensemble mean and no corresponding asymmetries in predictability. The CGCM, however, suggests that the spread is highly dependent on the ensemble mean with small spread for cold ENSO events and large spread for warm ENSO events. This result suggests that cold events may be more predictable than warm events with the CGCM. This is borne out in retrospective forecast experiments (Kirtman 2003).

The net result here is that there is significant coupled variability in the *COLA anomaly coupled model* in the tropical Indo-Pacific region that cannot be explained by a damped linear stochastically forced model. This does not imply that the stochastic forcing is unimportant; on the contrary, at a minimum it appears to be a significant contributor to the irregularity of ENSO and serves to modulate the periodicity. It is also possible that the assumption that the noise is linear is problematic; perhaps the noise should be multiplicative (A. Majda, personal communication). This result also does not imply that the damped linear theory is of no use in terms of understanding predictability. Indeed, the ensemble mean and spread relationship noted above applies to mature events where non-linearity is important. The damped linear theory is applicable to the growth of small perturbations (i.e., stochastic optimals), particularly as precursors to events as opposed to the mature phase of ENSO.

While these results may be model-dependant, the interactive ensemble procedure is universally applicable to any number of different AGCMs and OGCMs. It is a procedure that can systematically reduce the noise in the coupled system and can be used to diagnose the sources of climate variability. In addition, one interpretation of the interactive ensemble is that it is an effective way to perform idealized experiments that has only previously been possible in simplified theoretically motivated coupled models (E. Schneider personal communication). Finally, we note that the outstanding remaining challenge is to understand the important processes in Nature. In this regard, our best hope is to continue to improve the CGCMs and apply the interactive ensemble to additional models, and, perhaps, find agreement.

Acknowledgments: SMK was a summer intern at COLA while working on this project. BPK is indebted to E. Schneider, Z. Wu, T. DelSole, P. Schopf, J. Shukla, and J. Kinter all at COLA for valuable discussions. This research was supported by grants from the National Science Foundation ATM-9814295 and ATM-0122850, the National Oceanic and Atmospheric Administration NA16-GP2248 and the National Aeronautics and Space Administration NAG5-11656.

5. References

Barsugli, J., and D. S. Battisti, 1998: The basic effects of atmosphere-ocean thermal coupling on midlatitude variability. *J. Atmos. Sci*., **55**, 473-493.

Battisti, D. S., 1988: Dynamics and Thermodynamics of a Warming Event in a Coupled Tropical Atmosphere–Ocean Model. *Journal of the Atmospheric Sciences*, 45, 2889–2919.

Blanke, B., J. D., Neelin, and D. Gutzler, 1997: Estimating the Effect of Stochastic Wind Stress Forcing on ENSO Irregularity. *Journal of Climate*, **10**, 1473–1487.

Briegleb, B. P., 1992: Delta-Eddington approximation for solar radiation in the NCAR community climate model. *J. Geophys. Res.*, **97**, 7603-7612.

Chang, P., B. Wang, T. Li. and L. Ji, 1994: Interactions between the seasonal cycle and the Southern Oscillation-frequency entrainment and chaos in an intermediate coupled ocean-atmosphere model. *Geophys. Res. Lett.*, **21**, 2817-2820.

Chen, Y.-Q., D. S. Battisti, T. N. Palmer, J. Barsugli, and E. S. Sarachik, 1997: A Study of the Predictability of Tropical Pacific SST in a Coupled Atmosphere–Ocean Model Using Singular Vector Analysis: The Role of the Annual Cycle and the ENSO Cycle. *Mon. Wea. Rev.* **125**, 831–845.

DeWitt, D. G., 1996: The effect of the cumulus convection on the climate of the COLA general circulation model. COLA Tech. Rep. 27, 69 pp. [Available from COLA, 4041 Powder Mill Road, Suite 302, Calverton, MD 20705.]

DeWitt, D. G., and E. K. Schneider, 1996: The Earth radiation budget as simulated by the COLA GCM. COLA Tech. Rep. 35, 39 pp. [Available from COLA, 4041 Powder Mill Road, Suite 302, Calverton, MD 20705.]

Eckert, C., and M. Latif, 1997: Predictability of a Stochastically Forced Hybrid Coupled Model of El Niño. *Journal of Climate*, **10**, 1488–1504.

Fedorov, A. V., and S. G. H. Philander, 2001: A Stability Analysis of Tropical Ocean–Atmosphere Interactions: Bridging Measurements and Theory for El Niño. *J. Climate*, **14**, 3086–3101.

Flügel, M., and P. Chang, 1996: Impact of dynamical and stochastic processes on the predictability of ENSO. *Geophys. Res. Lett.*, **23**, 2089-2092.

Flugel, M., P. Chang, and C. Penland, 2004: The role of stochastic forcing in modulating ENSO predictability. *J. Climate* (in press).

Gent, P. R., and J. C. McWilliams, 1990: Isopycnal mixing is ocean circulation models. *J. Phys. Oceanography*, **25,** 150-155.

Harshvardhan, R. Davis, D. A. Randall and T. G. Corsetti, 1987: A fast radiation parameterization for general circulation models. *J. Geophys. Res*., **92**, 1009-1016.

Jin, F. F., J. D. Neelin, and M. Ghil, 1994: El Niño on the Devil's staircase: Annual subharmonic steps to chaos. *Science*, **264**, 70-72.

Jin, F.-F., 1997: An Equatorial Ocean Recharge Paradigm for ENSO. Part I: Conceptual Model. *J. Atmos. Sci.*, **54**, 811–829.

Kalnay, E., Kanamitsu, M., Kistler, R., Collins, W., Deaven, D., Gandin, L., Iredell, M., Saha, S., White, G., Woollen, J., Zhu, Y., Leetmaa, A., Reynolds, B., Chelliah, M., Ebisuzaki, W., Higgins, W., Janowiak, J., Mo, K.C., Ropelewski, C., Wang, J., Jenne, Roy, Joseph, Dennis. 1996: The NCEP/NCAR 40-Year Reanalysis Project. *Bul. Amer. Meteoro. Soc.*,**77,** 437–472.

Kiehl, J. T., J. J. Hack and B. P. Briegleb, 1994: The simulated Earth radiation budget of the National Center for Atmospheric Research community climate model CCM2 and comparisons with the Earth Radiation Budget Experiment (ERBE). *J. Geophys. Res.*, **99**, 20815-20827.

Kinter, J. L. III, J. Shukla, L. Marx and E. K. Schneider, 1988: A simulation of winter and summer circulations with the NMC global spectral model. *J. Atmos. Sci.*, **45**, 2468-2522.

Kinter, J. L. III, D. G. DeWitt, P. A. Dirmeyer, M. J. Fennessy, B. P. Kirtman, L. Marx, E. K. Schneider, J. Shukla and D. Straus, 1997: The COLA Atmosphere-Biosphere General Circulation Model Volume 1: Formulation. COLA Tech. Rep. 51, 46pp. [Available from COLA 4041 Powder Mill Road, Suite 302, Calverton, MD 20705.]

Kirtman, B. P., 1997: Oceanic Rossby wave dynamics and the ENSO period in a coupled model. *J. Climate*, **10**, 1690-1704.

Kirtman, B. P., and J. Shukla, 2000: Influence of the Indian summer monsoon on ENSO. *Quart. J. Roy. Meteor. Soc.*, **126**, 213-239.

Kirtman, Y. Fan and E. K. Schneider, 2002: The COLA global coupled and anomaly coupled ocean-atmosphere GCM. *J. Climate*, **15**, 2301-2320.

Kirtman, B. P., and J. Shukla, 2002: Interactive coupled ensemble: A new coupling strategy for GCMs. *Geophys. Res. Lett.*, **29**, 1029-1032.

Kirtman, B. P., 2003: The COLA anomaly coupled model: Ensemble ENSO prediction. *Mon. Wea. Rev.*, **131**, 2324-2341.

Kirtman, B. P., and P. S. Schopf, 1998: Decadal variability in ENSO predictability and prediction. *J. Climate*, **11**, 2804-2822.

Kirtman, B. P., J. Shukla, B. Huang, Z. Zhu and E. K. Schneider, 1997: Multiseasonal prediction with a coupled tropical ocean global atmosphere system. *Mon. Wea. Rev.*, **125**, 789-808.

Kleeman, R., and A. M. Moore, 1997: A Theory for the Limitation of ENSO Predictability Due to Stochastic Atmospheric Transients. *J. Atmos. Sci.*, **54**, 753–767.

Kleeman, R., Y. Tang, and A. M. Moore, 2003: The Calculation of Climatically Relevant Singular Vectors in the Presence of Weather Noise as Applied to the ENSO Problem. *J. Atmos. Sci.,* **60**, 2856–2868.

Large, W. G., J. C. McWilliams, and S. C. Doney, 1994: Oceanic vertical mixing: A review and a model with a nonlocal boundary layer parameterization. *Rev. of Geophys.*, **32,** 363-403.

Liess, S., L. Bengtsson, and K. Arpe: 2001: The Madden-Julian oscillation in the ECHAM4/OPYC3 CGCM. MPI Technical Report No. 319. [Available from MPI, Bundesstrasse 55, D-20146 Hamburg, Germany].

Mellor, G. L., and T. Yamada, 1982: Development of a turbulence closure model for geophysical fluid problems. *Rev. Geophys. Space. Phys*., **20**, 851-875.

Miyakoda, K., and J. Sirutis, 1977: Comparative integrations of global spectral models with various parameterized processes of sub-grid scale vertical transports. *Beitr. Phys. Atmos*., **50**, 445-480.

Moore, A. M., and R. Kleeman, 1996: The dynamics of error growth and predictability in a coupled model of ENSO. *Quart. J. Roy. Meteor. Soc*., **122**, 1405-1446.

Moore, A. M., and R. Kleeman, 1999a: The Non-normal Nature of El Niño and Intraseasonal Variability. *J. Climate*, **12** 2965–2982.

Moore, A. M., and R. Kleeman, 1999b: Stochastic forcing of ENSO by the intraseasonal oscillation. *J. Climate*, **12**, 1199-1220.

Moorthi, S., and M. J. Suarez, 1992: Relaxed Arakawa-Schubert: A parameterization of moist convection for general circulation models. *Mon. Wea. Rev*., **120,** 978-1002.

Munnich, M., M. A., Cane and S. E. Zebiak, 1991: A study of self excited oscillations in a tropical ocean-atmosphere system. Part II: Non-linear cases. *J. Atmos. Sci*., **48**, 1238-1248.

Pacanowski, R. C., and S. M. Griffies, 1998: MOM 3.0 Manual, NOAA/Geophysical Fluid Dynamics Laboratory, Princeton, USA 08542.

Penland, C., and L. Matrosova, 1994: A Balance Condition for Stochastic Numerical Models with Application to the El Niño-Southern Oscillation. *J. Climate*, **7**, 1352–1372.

Penland, C., and P. D. Sardeshmukh, 1995: The optimal growth of tropical sea surface temperature anomalies. *J.Climate*, **8**, 1999-2024.

Redi, M. H., 1982: Oceanic isopychnal mixing by coordinate rotation, *J. of Phys. Oceanogr*., **12**, 1155-1158.

Schneider, E. K., 2001: Causes of differences between the equatorial Pacific as simulated by two coupled GCM's. *J. Climate*, **15**, 2301-2320.

Smagorinsky, J., 1963: General circulation experiments with the primitive equations: I. The basic experiment. *Mon. Wea. Rev.,* **91,** 99-164.

Suarez, M. J., and P. S., Schopf, 1988: A Delayed Action Oscillator for ENSO. *J. Atmos. Sci*., **45**, 3283–3287.

Thompson, C. J., and D. S. Battisti, 2000: A Linear Stochastic Dynamical Model of ENSO. Part I: Model Development *J. Climate*, **13**, 2818-2832.

Thompson, C. J., and D. S. Battisti, 2001: A Linear Stochastic Dynamical Model of ENSO. Part II: Analysis. *J. Climate*, **14**, 445–466.

Trenberth, K. E., W. G. Large, and J. G. Olson, 1990: The mean annual cycle in global ocean wind stress. *J. Phys. Oceanogr*., **20**, 1742-1760.

Tziperman, E., M. A. Cane, and S. E. Zebiak, 1995: Irregularity and Locking to the Seasonal

Cycle in an ENSO Prediction Model as Explained by the Quasi-Periodicity Route to Chaos. *J. Atmos. Sci*., 52, 293–306.

Wang, B., Barcilon, A., Fang, Z. 1999: Stochastic Dynamics of El Niño–Southern Oscillation. *J. Atmos. Sci.*, 56, 5–23.

Wang, B., and X. Xie, 1997: A Model for the Boreal Summer Intraseasonal Oscillation. *J. Atmos. Sci*, **54**, 72–86.

Waliser, D. E., K. M. Lau, and J. H. Kim: 1999: The influence of coupled sea surface temperatures on the Madden-Julian oscillation: A model perturbation experiment. *J. Atmos. Sci.*, **56**, 333-358.

Wu, Z., E. K. Schneider and B. P. Kirtman, 2004: Causes of low frequency North Atlantic SST variability in a coupled GCM. *Geophys. Res. Lett.,* (in press).

Wu, R., and B. P. Kirtman, 2004c: Impact of Indian Ocean on the Indian summer Monsoon-ENSO Relationship. *J. Climate* (in press).

Wu, R., and B. P. Kirtman, 2004b: Understanding the impacts of the Indian Ocean on ENSO variability in a coupled GCM. *J. Climate* (in press).

Wu, R., and B. P. Kirtman, 2003: On the impacts of the Indian summer monsoon on ENSO in a coupled GCM. *Quart. J. Roy. Met. Soc*., **129**, 3439-3468.

Xue, Y., Cane, M. A., Zebiak, S. E.. 1997: Predictability of a Coupled Model of ENSO Using Singular Vector Analysis. Part I: Optimal Growth in Seasonal Background and ENSO Cycles. *Mon. Wea. Rev.,* **125**, 2043–2056.

Yeh, S.-W., and B. P. Kirtman, 2004c: Tropical decadal variability and ENSO amplitude modulation in a CGCM. *Climate Dyn.,* (submitted).

Yeh, S.-W., and B. P. Kirtman, 2004b: The low frequency variability of the tropical-North Pacific sea surface temperature teleconnections. *J. Climate* (submitted).

Yeh, S.-W., and B. P. Kirtman, 2004a: The impact of internal atmospheric variability on North Pacific decadal variability. *Climate Dyn*., (in press).

Zebiak, S.E., and M. A. Cane, 1987, A model El Niño-Southeren Oscillation. *Mon.Wea.Rev*., **115**, 2262-2278.

Zebiak, S. E., 1989: On the 30–60 Day Oscillation and the Prediction of El Niño. *Journal of Climate*, 2, 1381–1387.

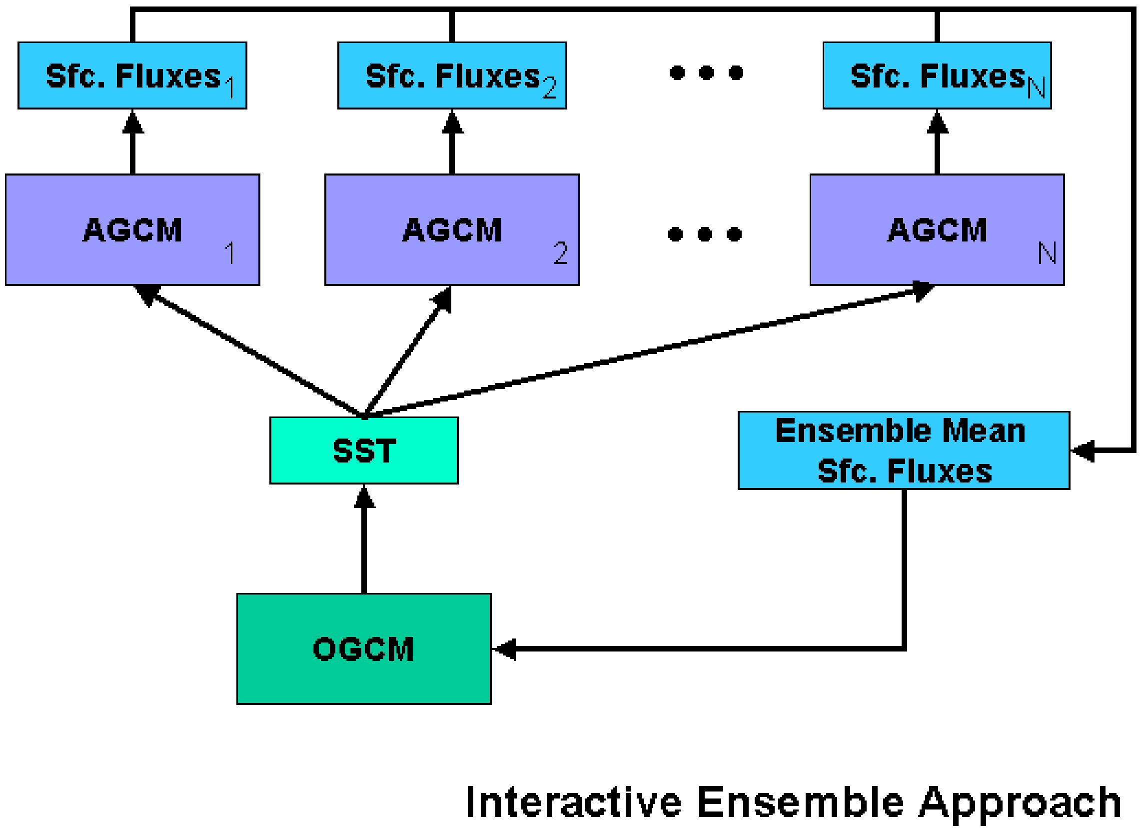

Figure 1: Schematic of the interactive ensemble approach.

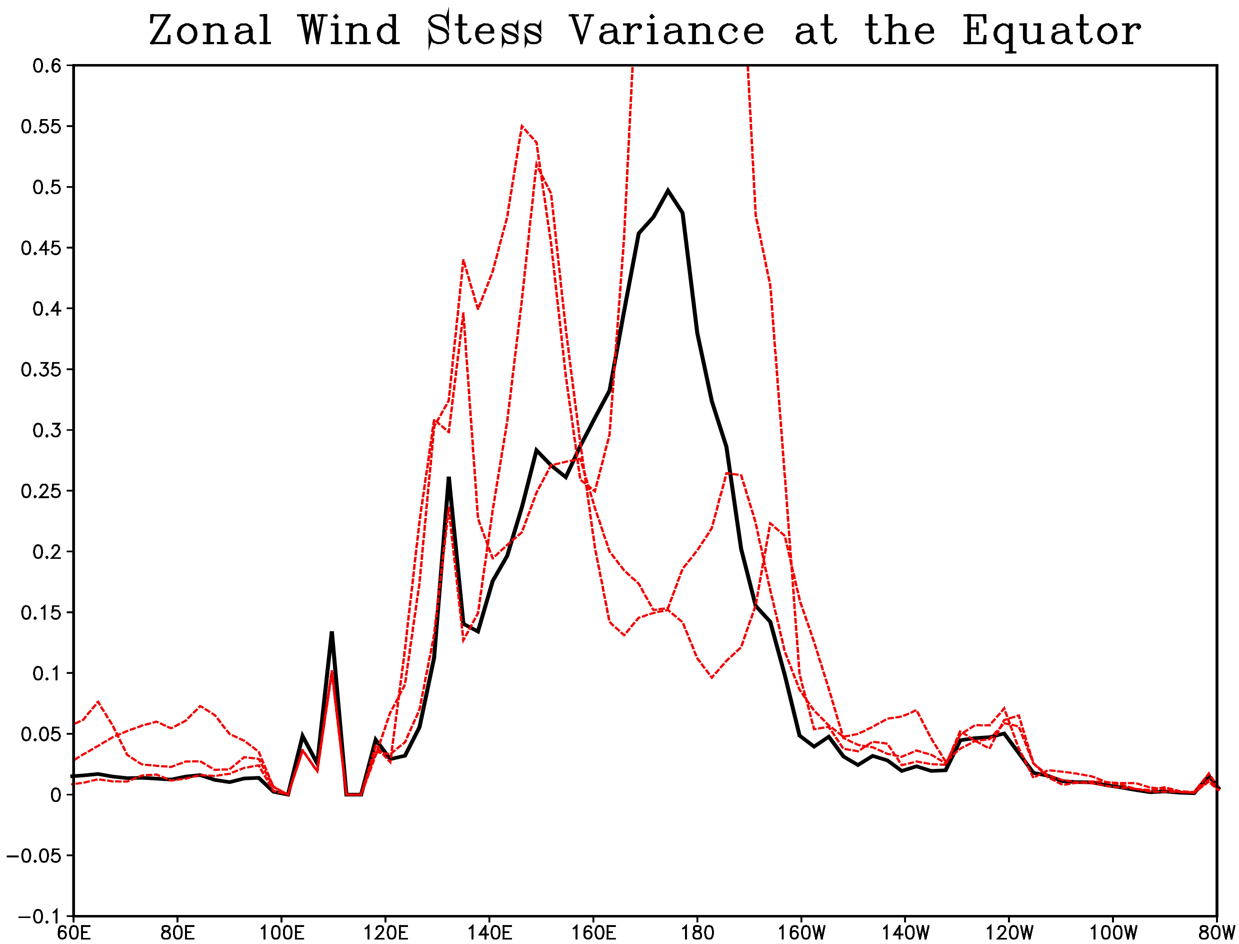

Figure 2: Zonal wind stress variance along the equator. The solid curve corresponds the ensemble mean variance (six-members) using daily data calculated over 1-yr. of an active El Niño. The dashed curves are the variance of six-day means from ensemble members 1, 3 and 5 calculated over the same year.

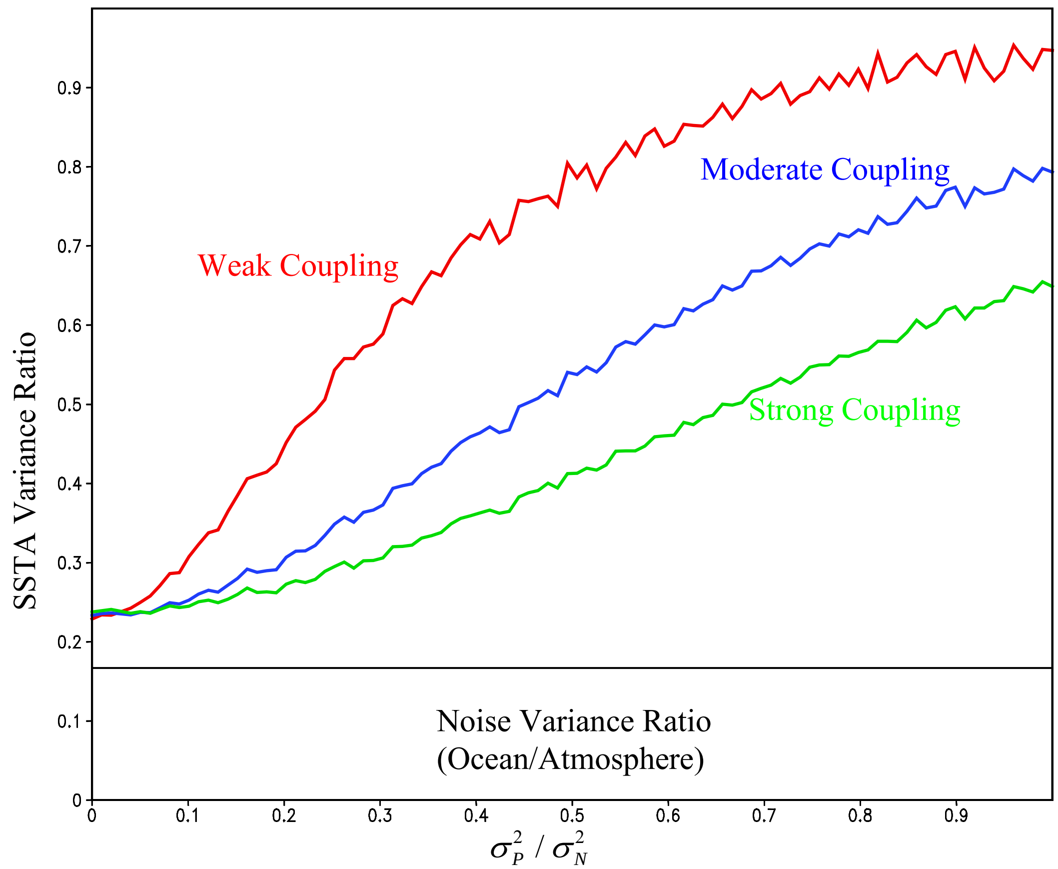

Figure 3: Heuristic coupled model SSTA variance ratio (interactive ensemble divided by standard coupling). The y-axis indicates the variance ratio and the x-axis indicate the ratio of ocean noise variance divided by atmosphere noise variance. The red curve corresponds to weak coupling (α=0.55, β=0.25), the blue curve indicates moderate coupling (α=0.55, β=0.5) and the green curve is for strong coupling (α=0.55, β=0.75). See text for details of the heuristic model.

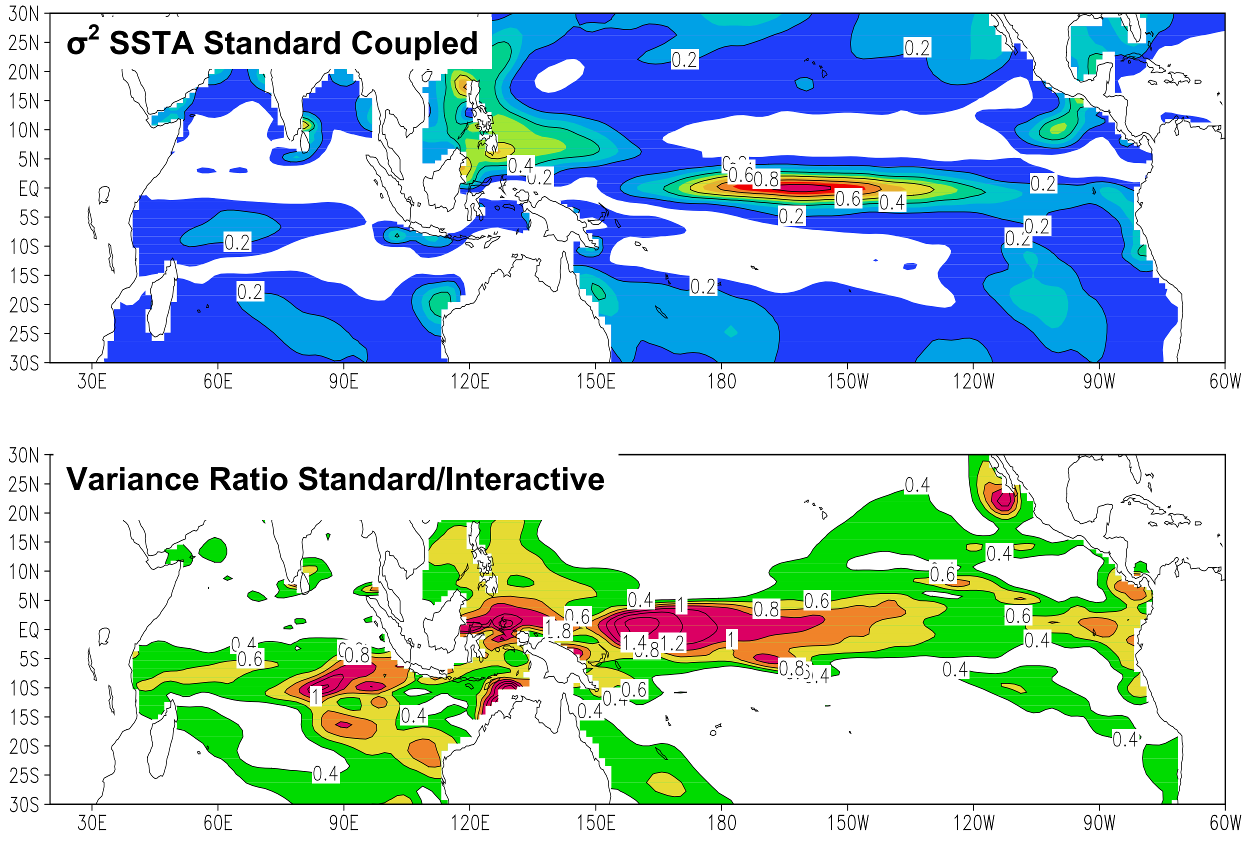

Figure 4: The top panel shows the SSTA standard deviation based on 100-years of data for the control CGCM. The contour interval is 0.2 $^oC^2$. The bottom panel shows the SSTA variance ratio for the interactive ensemble CGCM divided by the control CGCM. The contour interval is 0.2.

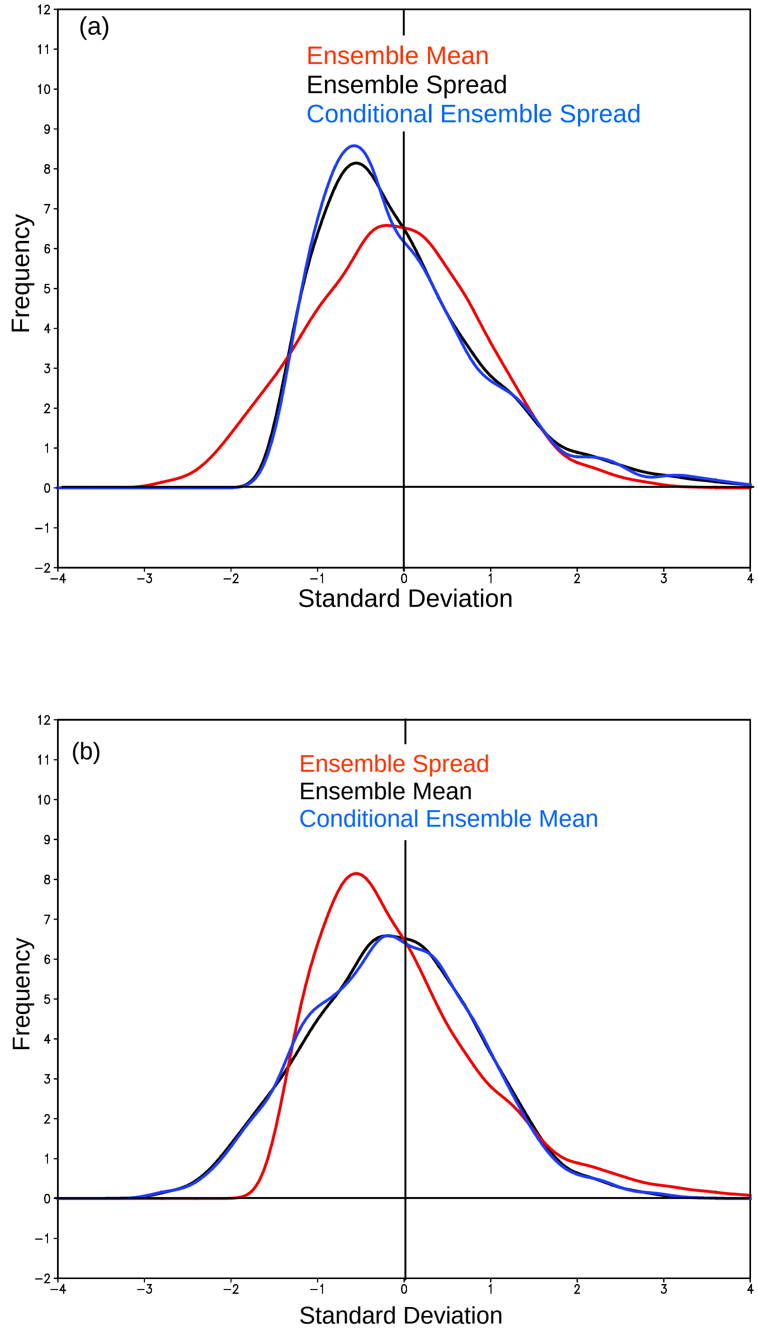

Figure 5: (a) Probability distribution function for the atmospheric component of the heuristic coupled model: ensemble mean (red), ensemble spread (black) and conditional ensemble spread (blue). (b) Probability distribution function for the atmospheric component of the heuristic coupled model: ensemble spread (red), ensemble mean (black) and conditional ensemble mean (blue).

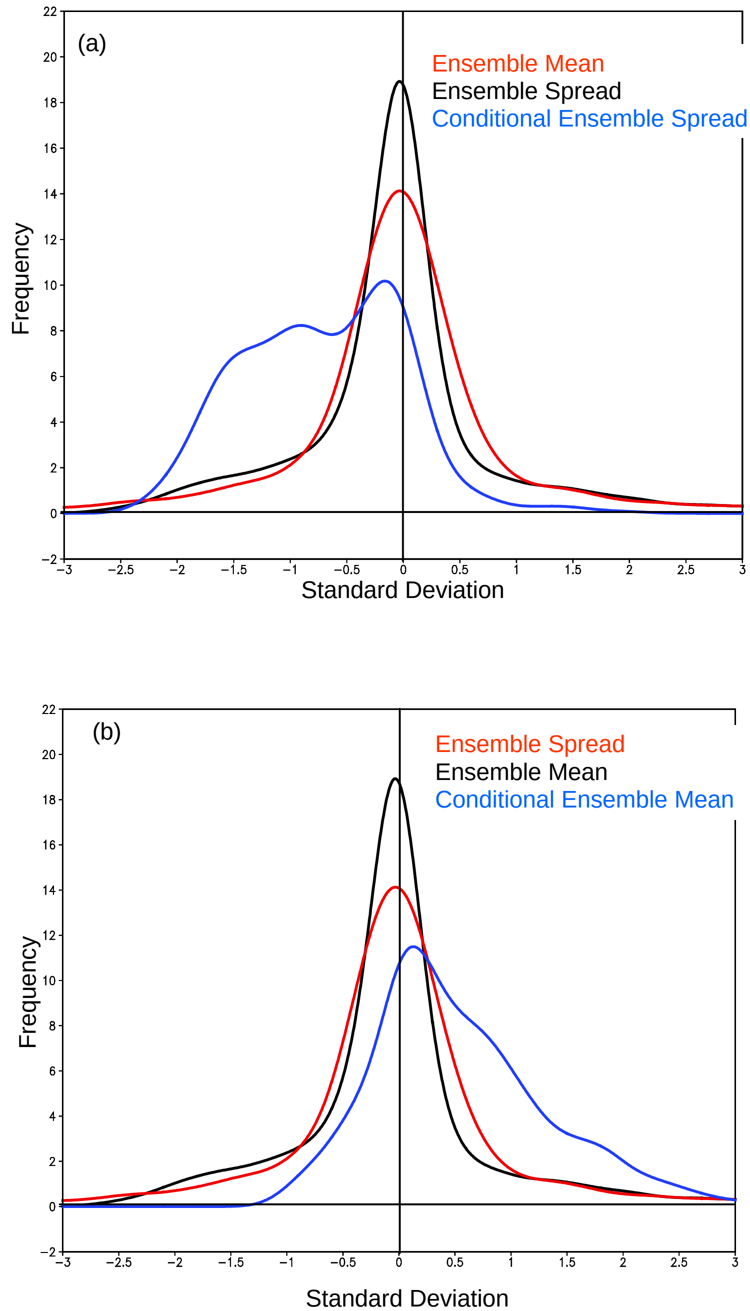

Figure 6: (a) Probability distribution function for the Nino4 zonal wind stress anomaly from the interactive ensemble CGCM: ensemble mean (red), ensemble spread (black) and conditional (mean easterlies) ensemble spread (blue). (b) Probability distribution function for the Nino4 zonal wind stress anomaly from the interactive ensemble CGCM: ensemble spread (red), ensemble mean (black) and conditional ensemble mean (blue).

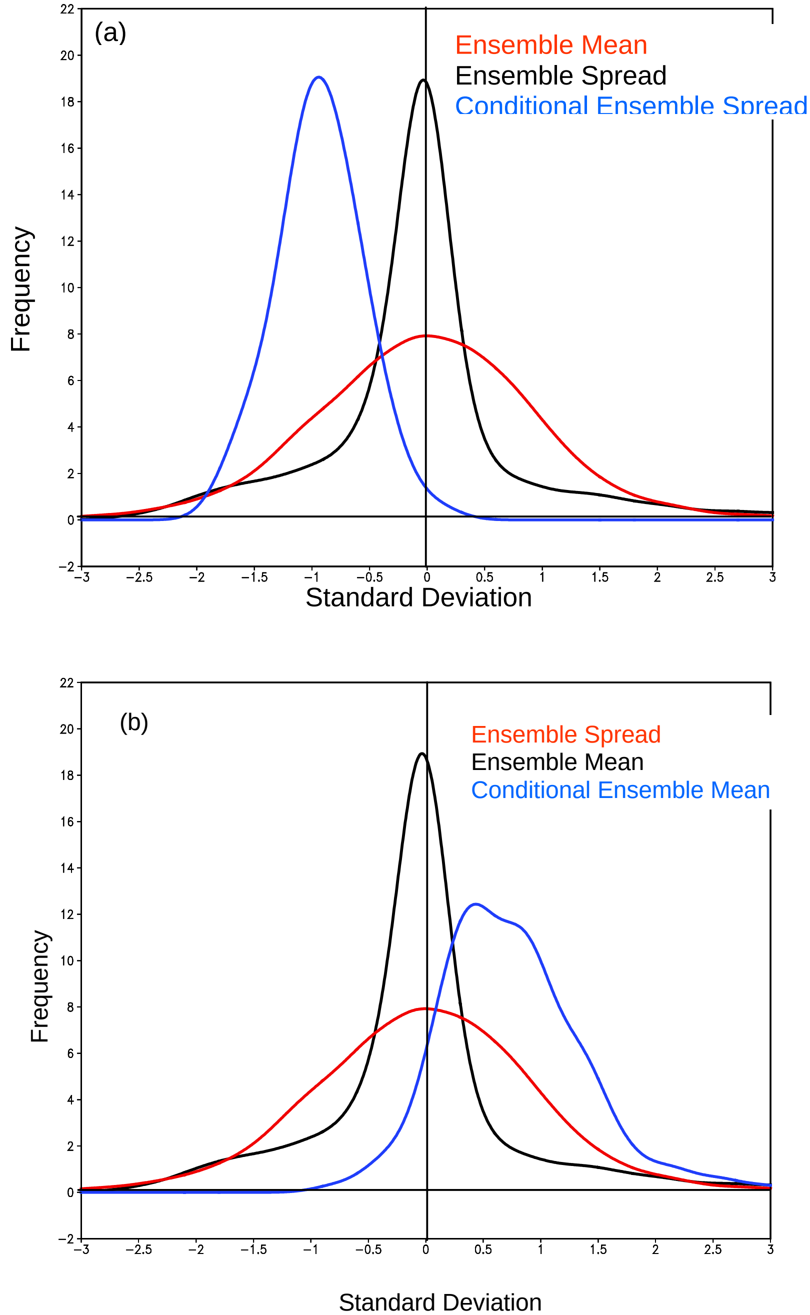

Figure 7: Interactive ensemble CGCM Probability density function for (a) the Nino3.4 SSTA (red), the zonal wind stress anomaly spread (black) and conditional (small spread) Nino3.4 SSTA (blue); (b) the Nino3.4 SSTA (red), the zonal wind stress anomaly spread (black) and conditional (large spread) Nino3.4 SSTA (blue).

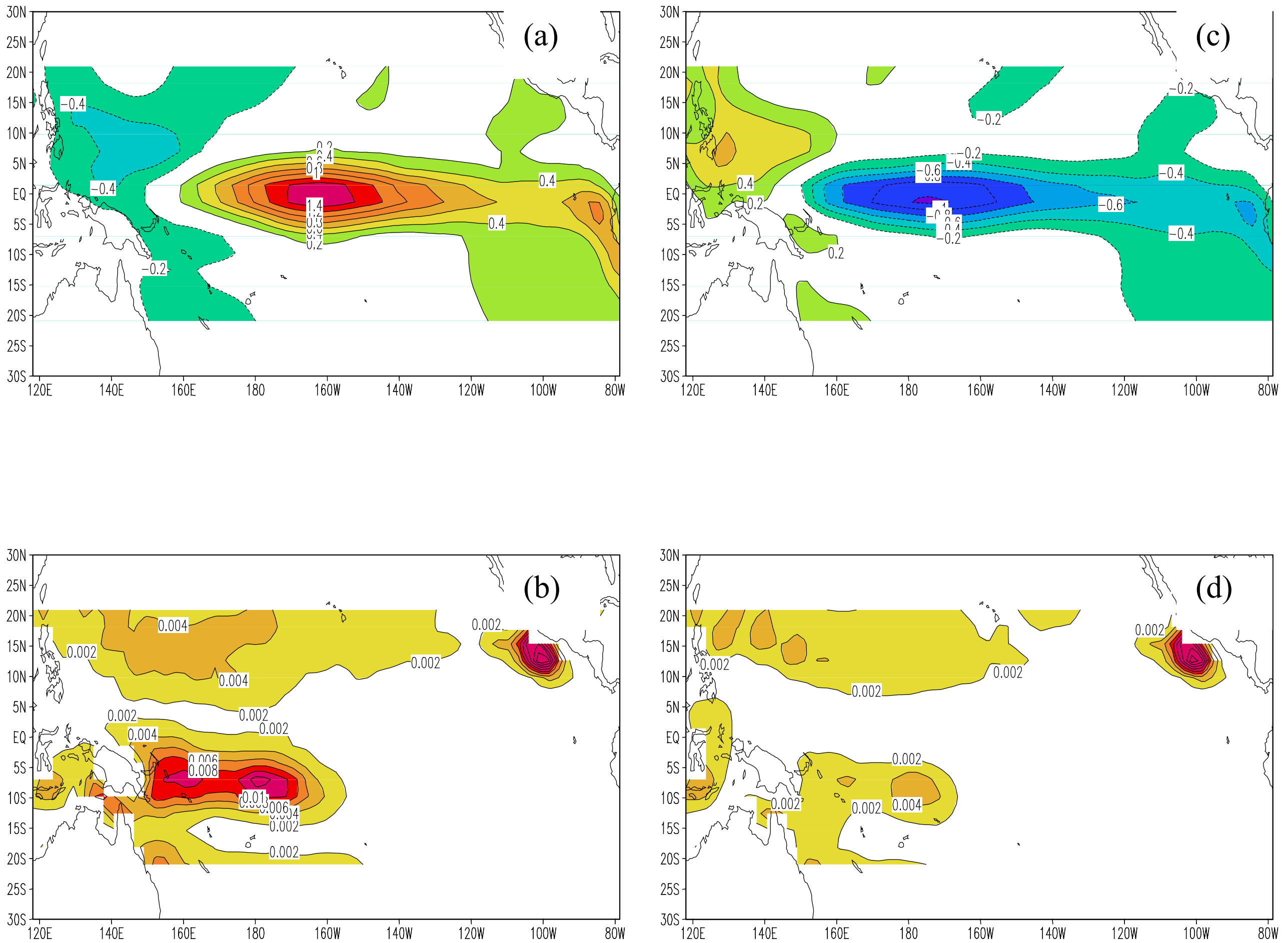

Figure 8: (a) SSTA composite of the top 5% of all simulated warm events measure by Nino3.4, (b) zonal wind stress spread composite based on the top 5% of all warm events, (c) SSTA composite of the top 5% of all simulated cold events measured by Nino3.4, and (d) zonal wind stress spread composite based on the top 5% of all cold events.

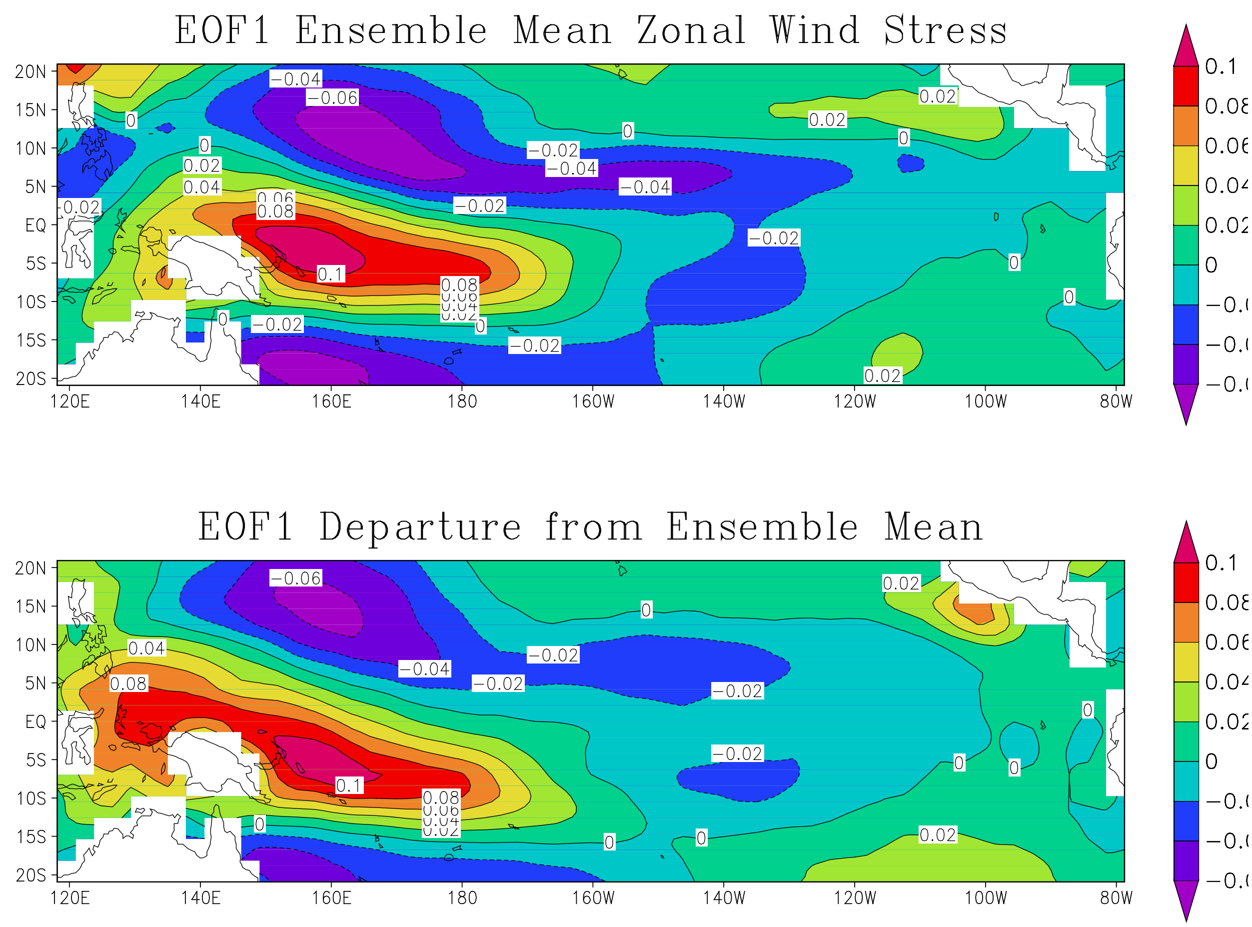

Figure 9: The top panel shows the first EOF of the ensemble mean zonal wind stress. The bottom panel shows the first EOF of the zonal wind stress deviation about the ensemble mean.